

# Fast Radio Bursts as cosmological proxies: estimating the Hubble constant

Eduard Fernando Piratova-Moreno,<sup>1\*</sup> Luz Ángela García,<sup>2</sup> Carlos A. Benavides-Gallego,<sup>3</sup> Carolina Cabrera<sup>1</sup>

<sup>1</sup>Fundación Universitaria Los Libertadores. Cra. 16 No. 63A-68, Bogotá, Colombia, Código Postal 111221

<sup>2</sup>Universidad ECCI, Cra. 19 No. 49-20, Bogotá, Colombia, Código Postal 111311

<sup>3</sup>School of Physics and Astronomy, Shanghai Jiao Tong University, 800 Dongchuan Road, Minhang, Shanghai 200240, PRC.

13 February 2025

## ABSTRACT

One of the most challenging problems in modern cosmology is the Hubble tension, a discrepancy in the predicted expansion rate of the Universe with different observational techniques that results in two conflicting values of  $H_0$ . We leverage the sensitivity of the Dispersion Measure (DM) from Fast Radio Bursts (FRBs) with the Hubble factor to investigate the Hubble tension. We build a catalog of 98 localized FRBs and an independent mock catalog and employ three methods to calculate the best value of the Hubble constant: i) the mean of  $H_0$  values obtained through direct calculation, ii) the maximum likelihood estimate (MLE), and iii) the reconstruction of the cosmic expansion history  $H(z)$  using two DM- $z$  relations previously explored in the literature. When the dataset of confirmed FRBs is employed, our predictions are compatible with reports from the Planck collaboration 2018, with  $H_0 = 65.13 \pm 2.52$  km/s/Mpc and  $57.67 \pm 11.99$  km/s/Mpc for maximum likelihood and the arithmetic mean, respectively. On the other hand, if we assume a linear and a power-law function for the DM- $z$  relation, our predictions for  $H_0$  are  $51.27^{+3.80}_{-3.31}$  km/s/Mpc and  $77.09^{+8.89}_{-7.64}$  km/s/Mpc, respectively. Finally, using 100 mock catalogs of 500 simulated FRBs in each realization, we obtain larger values for  $H_0$  with all methods considered:  $H_{0; \text{Like}} = 67.30 \pm 0.91$  km/s/Mpc,  $H_{0; \text{Mean}} = 66.21 \pm 3.46$  km/s/Mpc,  $H_{0; \text{Median}} = 66.10 \pm 1.89$  km/s/Mpc,  $H_{0; \text{Linear}} = 54.34 \pm 1.57$  km/s/Mpc and  $H_{0; \text{Power-law}} = 91.84 \pm 1.82$  km/s/Mpc for the MLE method, the arithmetic mean, and linear and power-law DM -  $z$  relations, respectively. More importantly, our results for mock FRB catalogs notably increase the statistical precision, ranging from 1.4% to 5.2% for the MLE method and arithmetic mean. In particular, our result with the MLE applied to synthetic FRBs is at the same level of precision as reports from SH0ES. Ultimately, the rapid increase in the number of confirmed FRBs will provide us with a robust prediction of the value of the Hubble constant, which, in combination with other cosmological observations, will allow us to alleviate (to a certain degree) the current Hubble tension.

**Key words:** Fast radio bursts – Cosmology – Hubble constant – Statistical methods – Transient.

## 1 INTRODUCTION

Fast Radio Bursts (FRBs) are bright millisecond transients detected in the radio waveband, ranging from 100 MHz to 8 GHz. Although their origin has not yet been discovered, nor the mechanisms that fuel these short bursts of energy, they have been depicted as having cosmological origin; therefore, they could be used to identify the properties of their galaxy hosts and the intergalactic medium through which their light goes before reaching our telescopes.

Besides the 2D angular coordinates, the main observable used to study FRBs is their dispersion measure (DM), which quantifies the properties of the medium where their light passes through, more specifically, the integrated number of free electrons along the path that interacts with their photons and causes a difference in the frequencies of light emitted by the object. This interaction between the FRB's photons and free electrons causes a difference between the radiation's highest and lowest frequencies, allowing us to infer the total DM.

Different authors have claimed that three components contribute to

the total  $DM_{\text{obs}}$  [Pol et al. \(2019\)](#); [Zhang et al. \(2020\)](#); [Zhu & Feng \(2021\)](#), among them, the dispersion due to our galaxy,  $DM_{\text{MW}}$ , and due to their extragalactic origin, a term due to the intergalactic medium (IGM),  $DM_{\text{IGM}}$ , and a third one caused by the interaction of the FRB photons with their host galaxy,  $DM_{\text{host}}$ . The second and third terms have intricate dependencies on redshift  $z$ , explained mainly by their cosmological origins. Although the modeling of each one of the latter terms is complex and constitutes an extensive field of study of FRBs.

To date, a few thousand FRBs have been detected, and the census is rapidly growing with the new radio telescopes that come online that observe and characterize these transients. Only a tiny fraction of these reported FRBs in the literature has direct information about their  $z$  because their galactic progenitors cannot be identified with radio observations; thus, other wavelength surveys need to observe the patch of the sky where the FRB is detected to have an inferred  $z$  and complete their localization. However, less than a hundred FRBs have been detected with known  $z$  (i.e., their hosting galaxy is identified), many of which are at low redshift.

Recent studies focus on modeling the relationship between the ob-

\* E-mail: efpiratovam@libertadores.edu.co

served DM and their corresponding  $z$ . For instance, [Macquart et al. \(2020\)](#); [Cui et al. \(2022\)](#); [Baptista et al. \(2023\)](#) presented different fits for a linear relation in DM vs.  $z$ . In particular, [Piratova-Moreno & García \(2024\)](#) presents a revision of different  $DM_{\text{obs}}$  models as a function of the redshift based on physical motivations. In the latter work, the authors used 24 FRBs with  $z$  known to propose different relations for  $DM_{\text{obs}}(z)$ : a linear trend, a log parabolic relation, a power-law model, and as a separate stage, an interpolation that not only takes into account  $z$ , but also the angular coordinates of each FRB, following results from [Xu et al. \(2021\)](#).

On the other hand, FRBs could offer a new window for cosmological studies because of their random distribution in the sky. Eventually, it will allow us to cross-correlate their position with galaxy redshift surveys. Despite the increasing number of cosmological FRBs, those with  $z \geq 0.5$ , there is an inner challenge in deriving cosmological parameters and delivering information about the state of the intergalactic medium through the study of the dispersion measure of these transients due to the small sample of identified FRBs. Nonetheless, astronomers can use a combined analysis with other cosmological observations, such as the luminosity distance of SNIa, inferred cosmology from the cosmic microwave background (CMB), Gamma Ray Bursts (GRB), Big Bang Nucleosynthesis (BBN), Baryon Acoustic Oscillations (BAO), among others, to derive solid constraints on the value of the fine-structure constant, the value of the baryon fraction  $\Omega_b$  (given the correlation with the number of free electrons calculated from the DM), the equation of state of the dark energy [Deng & Zhang \(2014\)](#); [Zheng et al. \(2014\)](#), and  $H_0$  (the Hubble constant measured today). Notably, FRB studies provide an independent method to calculate a value of  $H_0$ , which would benefit the astronomical community currently facing the so-called ‘‘Hubble tension’’ [Di Valentino et al. \(2021\)](#); [Kamionkowski & Riess \(2023\)](#); [Verde et al. \(2024\)](#). The Hubble tension invokes a large discrepancy between the values of  $H_0$  inferred from the CMB:  $67.4 \pm 0.5$  km/s/Mpc [Planck Collaboration et al. \(2020a\)](#), and a recent release of SNIa:  $73.0 \pm 1.0$  km/s/Mpc [Riess et al. \(2022\)](#), measured in the local universe from the SH0ES collaboration. Since the dispersion measure of the FRBs accounts for the distance between the transient and us, the DM is related to  $H_0$  through the Hubble parameter in a non-trivial way and, thus, can be used as a proxy to estimate  $H_0$ .

Different groups have started a campaign to derive values of  $H_0$  based on the current FRBs available. For instance, [Hagstotz et al. \(2022\)](#) reported a value of  $62.3 \pm 9.1$  km/s/Mpc using 12 FRBs. On the other hand, [Wu et al. \(2022\)](#) presented a final value of  $H_0 = 68.81^{+4.99}_{-4.33}$  km/s/Mpc using 18 localized FRBs with a theoretical approach. With the same number of FRBs, [Liu et al. \(2023\)](#) reported a value of  $71 \pm 3$  km/s/Mpc. Using 16 FRBs observed with ASKAP, [James et al. \(2022\)](#) reported a value of  $73^{+13}_{-8}$  km/s/Mpc. Moreover, [Zhao et al. \(2022\)](#) reported a  $H_0$  of  $80.4^{+24.1}_{-19.4}$  km/s/Mpc for the expansion rate today with 12 unlocalized FRBs and BBN constraints. Furthermore, [Wei & Melia \(2023\)](#) provided an estimate  $95.8^{+7.8}_{-9.2}$  km/s/Mpc, accounting for 24 reported FRBs with known  $z$ . [Hoffmann et al. \(2024\)](#) reported a value for  $H_0$  of  $64^{+15}_{-13}$  km/s/Mpc, making use of 26 selected FRBs from the DSA, FAST and CRAFT surveys. On the other hand, [Yang, Tsung-Ching et al. \(2025\)](#) reported  $H_0 = 74^{+7.5}_{-7.2}$  km/s/Mpc using 30 FRBs and the temporal scattering of the FRB pulses due to the propagation effect through the host galaxy plasma. Applying Monte Carlo simulation to 69 localized FRBs, [Gao et al. \(2024\)](#) presented a value of

Hubble constant  $70.41^{+2.28}_{-2.34}$  km/s/Mpc. Finally, [Wang et al. \(2025\)](#) performed an analysis combining 92 localized FRBs with data for DESI Y1, indicating a preference for a dynamical dark energy model  $\omega_0 - \omega_a$  over the  $\Lambda$ CDM standard model, and with the FRB subset-only, and values for  $H_0$  of  $69.04^{+2.30}_{-2.07}$  km/s/Mpc and  $75.61^{+2.23}_{-2.07}$  km/s/Mpc, assuming galactic electron density models NE2001 [Cordes & Lazio \(2002\)](#) and YMW16 (Yao et al. in prep), respectively.

In a similar fashion, we extend the catalog of FRBs presented in [Piratova-Moreno & García \(2024\)](#) to the latest 98 localized FRBs in the literature to perform a thorough statistical analysis and find a robust value for  $H_0$ . We use the maximum likelihood estimate (MLE) method and other statistical metrics to find the best value of  $H_0$  with the FRBs in the observed catalog. Then we calculate the value of  $H_0$  assuming two of the models explored in [Piratova-Moreno & García \(2024\)](#): the linear trend and the power-law function of the  $DM_{\text{obs}}$  with  $z$  and follow the evolution of  $H(z)$ , as explored in [Fortunato et al. \(2024\)](#). Finally, we build a synthetic catalog of FRBs (increasing the observed sample by a factor of 5) to derive the best-fit value of  $H_0$  with each one of the methods described with confirmed FRBs.

The outline of this work goes as follows: section 2 describes in detail how the different contributions to the dispersion measure (DM) are modeled. Section 3 is devoted to presenting our statistical analysis to retrieve the best values of  $H_0$  implementing three completely different methods and, the confirmed FRBs. Section 4 shows the analysis made with mock catalogs and presents the values obtained for the Hubble constant in this way. Finally, section 5 presents the main conclusions found in this work. Throughout the paper, we have assumed a flat  $\Lambda$ CDM model with cosmological parameters from [Planck Collaboration et al. \(2020a\)](#).

## 2 DISPERSION MEASURE (DM)

As Fast Radio Burst (FRB) signals travel toward Earth, they undergo dispersion, resulting in a time delay between the arrival of different frequencies. This delay is quantified using the dispersion measure (DM) as follows:

$$\Delta t \propto \left( \nu_{\text{lo}}^{-2} - \nu_{\text{hi}}^{-2} \right) \cdot \text{DM}, \quad (1)$$

with  $\nu_{\text{lo}}$  and  $\nu_{\text{hi}}$  are the lowest and highest frequencies of the emitted signal, respectively. The dispersion measure is associated with the column density of free electrons along the signal’s path and is expressed as:

$$\text{DM} = \int \frac{n_e}{(1+z)} dl, \quad (2)$$

where  $n_e$  is the cosmic free electron density, and  $l$  is the line of sight to the FRB. The observed dispersion measure ( $DM_{\text{obs}}$ ) is estimated from the following contributions:

$$DM_{\text{obs}} = DM_{\text{IGM}} + DM_{\text{MW}} + \frac{DM_{\text{host}}}{1+z}, \quad (3)$$

where the dispersion measure due to the Milky Way is  $DM_{\text{MW}}$ ;  $DM_{\text{IGM}}$ , the contribution of the intergalactic medium to the dispersion; and  $DM_{\text{host}}$ , corresponds to the contribution of the host galaxy.

## 2.1 Dispersion measure due to the Galaxy Host ( $DM_{\text{host}}$ ) and Milky Way ( $DM_{\text{MW}}$ )

We assume that the contribution from the host galaxy follows a similar form to that of the Milky Way, as:

$$DM_{\text{host}} = \frac{100}{1 + z_{\text{host}}} \text{ pc cm}^{-3}, \quad (4)$$

with an associated uncertainty given by Hagstotz et al. (2022):

$$\sigma_{\text{host}} = \frac{50}{1 + z_{\text{host}}} \text{ pc cm}^{-3}. \quad (5)$$

On the other hand, the contribution of the Milky Way ( $DM_{\text{MW}}$ ) has been estimated to range between 50-100  $\text{pc cm}^{-3}$  Prochaska & Zheng (2019), with a value of 100  $\text{pc cm}^{-3}$  selected for this work. The predicted DM values align with pulsar observations within an uncertainty of approximately  $\sigma_{\text{MW}} \sim 30 \text{ pc cm}^{-3}$  Manchester et al. (2005), which is adopted as the model's uncertainty estimate.

## 2.2 Intergalactic Medium Dispersion Measure ( $DM_{\text{IGM}}$ )

The contribution of the intergalactic medium to the dispersion measure can be expressed as follows:

$$DM_{\text{IGM}}(z) = \int_0^z n_e(z') f_{\text{IGM}}(z') \frac{1+z'}{H(z')} dz', \quad (6)$$

where  $H(z)$  is the Hubble parameter that intrinsically depends on  $H_0$  and  $z$ , and  $f_{\text{IGM}}$ , the baryon mass fraction. For the redshift range considered, where almost all baryons are ionized, the cosmic electron density can be approximated as a function of the baryon abundances:  $n_e(z) \approx \chi_e \frac{\bar{\rho}_b}{m_p}$  Hagstotz et al. (2022), where  $\bar{\rho}_b$  is the mean baryon density,  $m_p$  the proton mass, and the electron fraction  $\chi_e = Y_H + \frac{1}{2}Y_{He}$ . Assuming that the primordial abundances of Hydrogen and Helium satisfy the relationships  $Y_H \approx 1 - Y_{He}$  and  $Y_{He} = 0.24$ , as determined by CMB measurements Planck Collaboration et al. (2020b) and spectroscopic observations Aver et al. (2015),  $\chi_e \approx 1 - \frac{1}{2}Y_{He}$ . On the other hand, the fraction of electrons in the intergalactic medium,  $f_{\text{IGM}}$ , is calculated by subtracting the fraction bound in stars, compact objects, and dense interstellar medium (ISM). For the present analysis, we adopt  $f_{\text{IGM}} = 0.84$ , following Hagstotz et al. (2022).

With the previous considerations, the IGM contribution can be written as follows:

$$DM_{\text{IGM}}(z) = \frac{3c\Omega_b H_0}{8\pi G m_p} \chi_e f_{\text{IGM}} \int_0^z \frac{1+z'}{E(z')} dz'. \quad (7)$$

Here,  $\Omega_b$  is the dimensionless baryon density parameter and  $E(z)$  is the reduced Hubble factor defined as  $E(z) = \frac{H(z)}{H_0}$ , under the standard  $\Lambda$ CDM model. Since eq. (7) has a direct dependence on  $H_0$ , we can use it to calculate the value of this cosmological parameter. Finally, hydrodynamic simulations suggest an inhomogeneous distribution of electrons in the IGM, such a distribution can be effectively modeled by a Gaussian centered around the value provided by the equation (7). On the other hand, a linear interpolation of the uncertainties is applied between the values reported by the simulations, specifically  $\sigma_{\text{IGM}}(z=0) \approx 40 \text{ pc cm}^{-3}$  and  $\sigma_{\text{IGM}}(z=1) \approx 180 \text{ pc cm}^{-3}$  Hagstotz et al. (2022).

## 3 CALCULATING $H_0$ WITH OUR FRB CATALOG

This section presents three methods for estimating  $H_0$  using localized FRB data in Table A1. FRB221027A is excluded for its am-

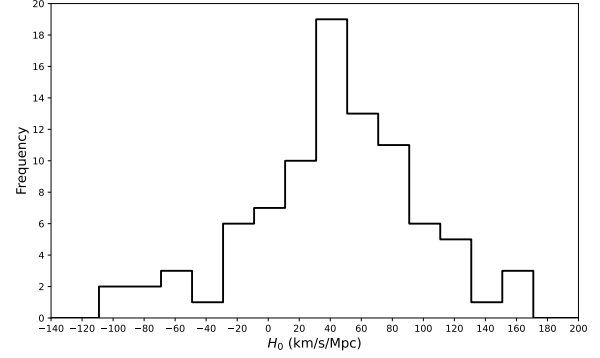


**Figure 1.** The histogram represents the frequency distribution of  $H_0$  values derived from the data. Using the arithmetic mean, the value for the Hubble constant with 97 confirmed FRBs is  $H_0 = 57.67 \pm 11.99 \text{ km/s/Mpc}$ .

biguity in host galaxy localization, so we calculate with 97 FRBs. In the first method, the mean value obtained for  $H_0$  is based on the sensitivity of the IGM term to this parameter. The second method focuses on maximizing the likelihood function, while the third one derives from an expression for the cosmic expansion history,  $H(z)$ , and evaluates it at  $z = 0$ .

### 3.1 $H_0$ derived with the arithmetic mean

We can use equation (7) to calculate  $H_0$  for each localized FRB presented in Table A1 and then obtain the arithmetic mean of the data set. To this purpose, we substitute each contribution to DM discussed in Section 2 into eq. (3), such that:

$$DM_{\text{obs}} = \frac{3c\chi_e f_{\text{IGM}} \cdot 10^4 \Omega_b h^2}{8\pi G m_p H_0} \int_0^z \frac{1+z'}{E(z')} dz' + DM_{\text{MW}} + \frac{DM_{\text{host}}}{1+z}. \quad (8)$$

From eq. (8),  $H_0$  can be derived as:

$$H_0 = \frac{3c\chi_e f_{\text{IGM}}}{8\pi G m_p} \frac{10^4 \Omega_b h^2}{DM_{\text{obs}} - DM_{\text{MW}} - \frac{DM_{\text{host}}}{1+z}} \int_0^z \frac{1+z'}{E(z')} dz'. \quad (9)$$

The computed values of  $H_0$  with 97 FRBs in Table A1 are displayed in Figure 1. For each presented value in the histogram, we compute the error using error propagation as follows:

$$\sigma_{H_0} = \sqrt{\sum_{i=1}^n \left( \frac{\partial H_0}{\partial x_i} \cdot \sigma_{x_i} \right)^2}, \quad (10)$$

where  $x_i$  represents each of the variables that contribute to the propagation of errors and  $\sigma_{x_i}$  its errors, which in this case are:  $DM_{\text{obs}}$ ,  $DM_{\text{MW}}$ ,  $DM_{\text{host}}$  and  $z$ . The value for  $H_0$  obtained through this method is:

$$H_0 = 57.67 \pm 11.99 \text{ km/s/Mpc}. \quad (11)$$

Figure 2 displays the result in equation (11) in addition with the  $H_0$  values reported from the Planck Collaboration et al. (2020a) and SH0ES measurements Riess et al. (2022). Up to a precision of  $\sigma = 11.99 \text{ km/s/Mpc}$ , our result is compatible with Planck Collaboration et al. (2020a) data, and excludes in  $1\sigma$  SH0ES measurements Riess et al. (2022). However, as evident from Figure 2, a statistical precision of  $\approx 21\%$  is extremely low. Nevertheless, as we will demonstrate later with mock catalogs, it is expected that with a few hundred data points,

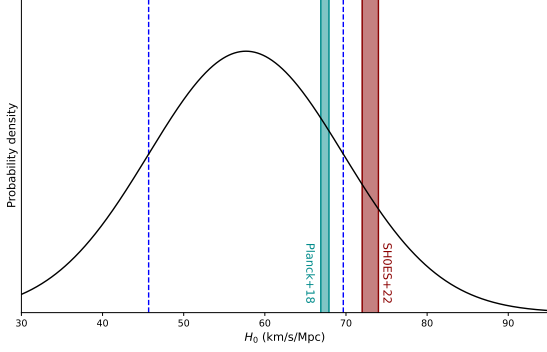


**Figure 2.** The Gaussian distribution obtained from the direct calculation and its associated errors is compared with the values reported by the [Planck Collaboration et al. \(2020a\)](#) and [Riess et al. \(2022\)](#) measurements. The blue dotted lines are the errors estimated as one standard deviation.

our predictions for  $H_0$  and its statistical precision will improve, and our forecast of this cosmological parameter will be more consistent with the values reported by the referred collaborations.

### 3.2 $H_0$ from cosmic expansion history

In this section, we discuss and apply a method to reconstruct the cosmic expansion history through the Hubble parameter  $H(z)$  and estimate its value today, i.e.,  $H_0$ . We remind the reader that we use the sample of localized FRBs in [Table A1](#), and, models first introduced in [Pirato-Moreno & García \(2024\)](#).

The Hubble parameter, redshift, and the mean dispersion measure of IGM for FRBs are interrelated through the equation (7). We obtain an explicit expression for  $H(z)$  by deriving it [Fortunato et al. \(2024\)](#):

$$H(z) = \frac{3c10^4\Omega_b h^2}{8\pi G m_p} \chi_e f_{\text{IGM}}(1+z) \left( \frac{d\text{DM}_{\text{IGM}}}{dz} \right)^{-1}. \quad (12)$$

Equation (12) can be used to reconstruct the cosmic expansion history,  $H(z)$ , considering the derivative of  $\text{DM}_{\text{IGM}}$  with respect to  $z$  and using the latter to estimate  $H_0$  as shown in [Liu et al. \(2023\)](#) and more recently in [Fortunato et al. \(2024\)](#). The models presented in [Pirato-Moreno & García \(2024\)](#) for 24 known FRBs (at the moment) have been updated to 97 in [Table A1](#). Among the models originally discussed in [Pirato-Moreno & García \(2024\)](#), only two have been considered in this work due to their superior performance when predicting  $z$  from the observed DM: the linear and power-law models. From eq. (3),  $\text{DM}_{\text{IGM}}$  is given by:

$$\text{DM}_{\text{IGM}} = \text{DM}_{\text{obs}} - \text{DM}_{\text{MW}} - \frac{\text{DM}_{\text{host}}}{1+z} \quad (13)$$

If the relationship between  $\text{DM}_{\text{obs}}$  and  $z$  is linear, as the Macquart relation [Macquart et al. \(2020\)](#); [Pirato-Moreno & García \(2024\)](#):

$$\text{DM}_{\text{obs}} = az + b, \quad (14)$$

with our sample of 97 FRB data points, the best-fit parameters for the linear trend are:  $a = 959.32 \pm 73.12 \text{ pc cm}^{-3}$  and  $b = 240.11 \pm 25.67 \text{ pc cm}^{-3}$ .

Now, if the DM- $z$  relationship is a the power-law function [Pirato-Moreno & García \(2024\)](#),  $\text{DM}_{\text{obs}}$  is modeled as:

$$\text{DM}_{\text{obs}} = A(1+z)^\alpha. \quad (15)$$

The updated values of  $A$  and  $\alpha$  our 97 localized FRBs are:  $A = 297.25 \pm 17.90 \text{ pc cm}^{-3}$ , and  $\alpha = 2.03 \pm 0.13$ .

Using the relationships (14) and (15) and the updated values for the free parameters in each case, the derivative  $\frac{d\text{DM}_{\text{IGM}}}{dz}$  can be obtained and substituted into the eq. (12). The Hubble parameter with our linear model is given by:

$$\frac{H(z)}{1+z} = \frac{3c}{8\pi G m_p} 10^4 \Omega_b h^2 f_{\text{IGM}}(z) f_e(z) \left[ 959.32 + \frac{100}{(1+z)^2} \right]^{-1}, \quad (16)$$

and equivalently, for our power-law function:

$$\frac{H(z)}{1+z} = \frac{3c}{8\pi G m_p} 10^4 \Omega_b h^2 f_{\text{IGM}}(z) f_e(z) \left[ 604.48(1+z)^{1.03} + \frac{100}{(1+z)^2} \right]^{-1} \quad (17)$$

By setting  $z = 0$  in equations (16) and (17), we recover a value for the Hubble constant today  $H_0 = 51.27^{+3.80}_{-3.31} \text{ km/s/Mpc}$  for the linear model, and  $H_0 = 77.09^{+8.89}_{-7.64} \text{ km/s/Mpc}$  for the power-law function, with statistical precisions of 7.4% and 11.5%, respectively.

In this case, the prediction of the linear model is inconsistent both with [Planck Collaboration et al. \(2020a\)](#) and [Riess et al. \(2022\)](#), but privileges lower values of  $H_0$ . On the other hand, the prediction of the power-law model is comparable with SH0ES measurements within the error range. Interestingly, the linear trend (also known as the Macquart relation) is extensively applied at the low  $z$  regime, but it leads to a poor prediction of  $H_0$  with our current census of FRBs.

### 3.3 $H_0$ from Maximum Likelihood Estimate (MLE).

This section is devoted to estimating the best-fit value of  $H_0$  when we maximize the Likelihood function with data in [Table A1](#). The likelihood function quantifies how well a given model of  $H_0$  explains the observed data, accounting for uncertainties in the measurements. This function is defined as:

$$\ln \mathcal{L}(H_0) = -\frac{1}{2} \sum_i \left[ \frac{(\text{DM}_{\text{obs};i} - \text{DM}_{\text{model};i})^2}{\sigma_i^2} + \ln(\sigma_i^2) \right] \quad (18)$$

where  $\text{DM}_{\text{obs}}$  represents the total dispersion measure,  $\text{DM}_{\text{model}}$  is the theoretical prediction dependent on  $H_0$ , and  $\sigma$  encompasses the total uncertainty, including contributions from the host galaxy, intergalactic medium, and Milky Way shown in section 2.

Our computation involves several steps: first, the log-likelihood is computed for a range of  $H_0$  values using the theoretical dispersion measure model  $\text{DM}_{\text{model}}(z, H_0)$ , which incorporates contributions from the intergalactic medium, host galaxies, and the Milky Way. Uncertainties are propagated through a quadratic sum to account for variability in each component:

$$\sigma_i = \sqrt{\sigma_{\text{MW}}^2(z_i) + \sigma_{\text{host}}^2(z_i) + \sigma_{\text{LSS}}^2(z_i)}. \quad (19)$$

The value of  $H_0$  that maximizes the log-likelihood corresponds to the most probable estimate of the Hubble constant given the data, and it is identified by locating the peak of the likelihood function. The uncertainty in  $H_0$  is estimated by calculating the second derivative of the log-likelihood at its maximum, with the error given by:

$$\sigma_{H_0} = \sqrt{\frac{1}{-\ln \mathcal{L}''(H_{0;\text{best}})}}, \quad (20)$$

where  $\ln \mathcal{L}''(H_{0;\text{best}})$  represents the second derivative of the

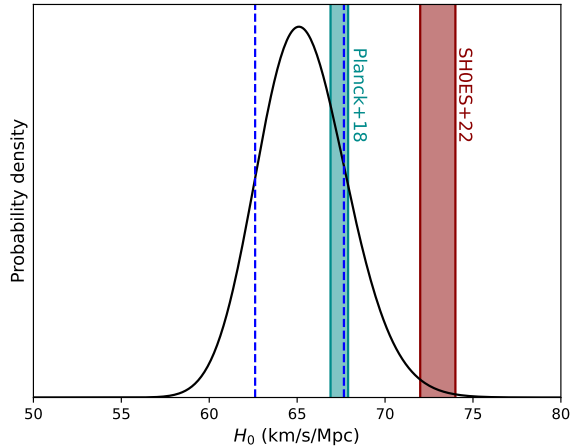


**Figure 3.** Posterior probability density function for  $H_0$  with 97 localized FRBs. Our best-fit value with the MLE method is  $H_0 = 65.13 \pm 2.52$  km/s/Mpc. Within the error margin (blue dotted lines), this prediction is compatible with other indirect methods, such as the one presented in [Planck Collaboration et al. \(2020a\)](#).

log-likelihood evaluated at the maximum.

To incorporate theoretical constraints, a rectangular prior is assumed in a range of [40, 100] for  $H_0$ , assigning a uniform probability density within this interval. The posterior distribution is constructed by multiplying the likelihood function by this prior. The peak of the posterior represents the combined (best) estimate of  $H_0$ . Using the MLE method, the best fit value for  $H_0$  is:

$$H_0 = 65.13 \pm 2.52 \text{ km/s/Mpc.} \quad (21)$$

The value reported in (21) has a statistical precision of 3.9%, significantly better than that obtained in the previous section using the arithmetic mean. Thus, our implementation of the MLE exhibits superior performance compared with the methods discussed in previous sections. Finally, the estimated value of  $H_0$  is compatible with the early universe prediction [Planck Collaboration et al. \(2020a\)](#) and disfavors the predicted value by [Riess et al. \(2022\)](#).

#### 4 FUTURE PROSPECTIVES WITH FRBS MOCK DATA

Currently, the available set of confirmed FRBs is limited; however, it is possible to simulate data to gain insight into the potential of these methods.

Following the procedure proposed in [Yu, H. & Wang, F. Y. \(2017\)](#); [Liu et al. \(2023\)](#); [Fortunato et al. \(2024\)](#), we adopt a flat  $\Lambda$ CDM model as the fiducial model, with the following cosmological parameters:  $H_0 = 70$  km/s/Mpc,  $\Omega_b = 0.049$ ,  $\Omega_m = 0.3$ , and  $\Omega_\Lambda = 1 - \Omega_m$ . Furthermore, we assume that the redshift distribution is described by  $f(z) \approx z^2 \exp(-\alpha z)$ , with  $\alpha = 7$  [Hagstotz et al. \(2022\)](#), a parameter that determines the depth of the simulated sample, acting as a filter that places most of the data points within the range  $z = 0.15 - 0.5$  consistent with confirmed data to-date.

The  $DM_{\text{IGM}}$  term is proposed through a normal distribution  $N(\langle DM_{\text{IGM}}^{\text{fid}} \rangle, \sigma_{DM_{\text{IGM}}^{\text{fid}}})$ , where  $\sigma_{DM_{\text{IGM}}^{\text{fid}}} = \sigma_{\Delta\text{IGM}}(z)$ . The term  $\langle DM_{\text{IGM}}^{\text{fid}} \rangle$  is calculated in eq. (7). The large dispersion of the values

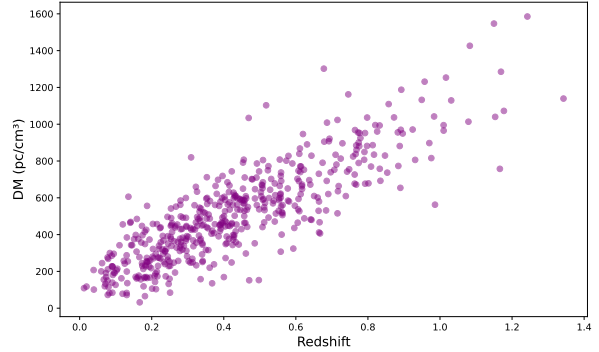


**Figure 4.** Reconstruction of the dispersion measure and redshift for one realization out of the 100 mock datasets.

Method	$H_0$ (km/s/Mpc)	Statistical precision (%)	
Arithmetic mean	$66.21 \pm 3.46$	5.2	
Median	$66.10 \pm 1.89$	2.9	
MLE	$67.30 \pm 0.91$	1.4	
$H(z)$	Linear model	$54.34 \pm 1.57$	2.9
	Power-law model	$91.84 \pm 1.82$	2.0

**Table 1.** Value of  $H_0$  in the different methods using 100 mock catalogs with 500 synthetic data each.

of  $DM_{\text{IGM}}$  around its mean value  $\langle DM_{\text{IGM}} \rangle$  is due to the inhomogeneity of the distribution of baryons in the intergalactic medium is modeled by with a power-law function presented in [McQuinn \(2013\)](#); [Qiang & Wei \(2020\)](#); [Fortunato et al. \(2024\)](#):

$$\sigma_{\Delta\text{IGM}}(z) = 173.8 z^{0.4} \text{ pc cm}^{-3}. \quad (22)$$

The contribution of the host galaxy is described by a log-normal distribution, such that:

$$P(DM_{\text{host}}) = \frac{1}{DM_{\text{host}} \sigma_{\text{host}} \sqrt{2\pi}} \exp\left(-\frac{(\ln(DM_{\text{host}}/\mu))^2}{2\sigma_{\text{host}}^2}\right). \quad (23)$$

Here,  $\mu$  is the geometric mean, and we consider it within the range [40, 80]  $\text{pc cm}^{-3}$ . The term  $\sigma_{\text{host}}$  is within the interval [0.4, 1.0].

We generate 100 independent realizations from random seeds between 0 and 199. Each set contains 500 simulated FRBs. We display one example of these synthetic samples in Figure 4. For each realization, we calculate a value of  $H_0$  applying the methods described in previous sections, such that we recover a set of 100 different values for  $H_0$ . Finally, we calculate the arithmetic mean and standard deviation for all these  $H_0$  values, which yields the results shown in Table 1.

The arithmetic mean is highly sensitive to the tails of the data distribution. In contrast, an analysis using the median proves to be more robust with an improvement in a factor of  $\sim 2$  in the statistical precision. The median value is only computed for our simulated dataset since it has proven this metric is more robust with large datasets. The median leads to a value for the Hubble parameter today of  $66.10 \pm 1.89$  km/s/Mpc, which is highly consistent with the prediction of [Planck Collaboration et al. \(2020a\)](#) but with lower statistical precision (2.9%) compared to arithmetic mean. The error reported for the median is the median absolute deviation (MAD).

For all methods applied in synthetic data, the values of  $H_0$  increase compared with those found with our catalog of 98 observed

FRBs, suggesting that with the current detected set of transients, the value of the Hubble constant might be underestimated, as indicated by the results in this section. The statistical precision will continue to improve as more confirmed data become available. On the other hand, our prediction using the arithmetic mean as a metric remains considerably high compared to the other methods, indicating that it would require more data to reliably estimate  $H_0$ . The best performance is achieved through the implementation of the MLE method, with values from  $65.13 \pm 2.52$  km/s/Mpc (statistical precision  $\sim 3.9\%$ ) calculated with the 97 FRBs in Table A1 and  $67.30 \pm 0.91$  km/s/Mpc (statistical precision 1.4%) for our synthetic dataset. In summary, the statistical precision improves by a factor of 2.8 when new data is used as input in our calculations. The statistical precision in the mock-case is comparable to the precision reported by the SH0ES collaboration. On the other hand, methods based on the reconstruction of  $H(z)$  exhibit the largest deviations from the values reported in Planck Collaboration et al. (2020a) and Riess et al. (2022). Notably, our prediction with the median value has a statistical precision similar to the methods based on  $H(z)$  but it is compatible with the value of  $H_0$  reported by Planck Collaboration et al. (2020a).

## 5 CONCLUSIONS

The Hubble constant ( $H_0$ ) is a very important cosmological parameter that measures the rate of expansion of the universe at current times. The so-called ‘‘Hubble tension’’ is the discrepancy with a gap of more than  $5\sigma$  between the predictions of  $H_0$  values by early Planck Collaboration et al. (2020a) and late Riess et al. (2022) universe observations. Fast radio bursts (FRBs) offer new pathways to quantify this cosmological parameter. In particular, it can be used to address the Hubble tension based on the sensitivity of the dispersion measure, in particular, in the IGM term. We construct a data set with 98 localized FRBs from literature and explore three different methods to estimate  $H_0$  value with 97 of them: i) arithmetic mean, ii) reconstruction of  $H(z)$  and iii) the Maximum Likelihood Estimate.

In the first method, based on the sensitivity of the intergalactic medium’s dispersion measure ( $DM_{\text{IGM}}$ ) to the Hubble constant,  $H_0$  is calculated using the 97 FRB data points in the catalog and its errors (Table A1). Using these data, we calculate a representative value as the arithmetic mean, with its associated error estimated through error propagation, yielding  $H_0 = 57.67 \pm 11.99$  km/s/Mpc, with a statistical precision of 20.7%. This result shows agreement with results from Planck Collaboration et al. (2020a).

In the second method, the cosmic expansion history  $H(z)$  is reconstructed by taking the derivative of the average value  $DM_{\text{IGM}}$  with respect to  $z$ . Two  $DM$ - $z$  relations are considered for calculating the derivative: a linear and a power-law function. These relationships are fitted using the 97 confirmed data points. Once  $H(z)$  is reconstructed, we set  $z = 0$  to recover  $H_0$ . The linear function leads to a value of  $H_0$  of  $51.27^{+3.80}_{-3.31}$  km/s/Mpc, closer to reports by Planck Collaboration et al. (2020a), with a statistical precision of 7.4%. On the other hand, unlike previous results, the power-law model predicts a higher value than Riess et al. (2022),  $77.09^{+8.89}_{-7.64}$  km/s/Mpc. However, it exhibits lower statistical precision than the linear model, at 11.5% level.

Finally, we use the MLE method to determine the best value of  $H_0$  that fits the proposed model to the 97 localized FRBs. This method achieves the best statistical precision at 3.9%, predicting a value for the Hubble parameter today of  $H_0 = 65.13 \pm 2.52$  km/s/Mpc. The

latter result is compatible with reports that use data from the early universe Planck Collaboration et al. (2020a).

Overall, our results with observed data have lower statistical precision compared to Planck Collaboration et al. (2020a); Riess et al. (2022). However, the number of FRBs with confirmed host galaxies is expected to increase significantly shortly. Therefore, it seems promising to evaluate these methods with larger datasets. To this end, we generate 100 mock catalogs with 500 data points each. We assume a particular redshift distribution discussed in section 4, a normal distribution for  $DM_{\text{IGM}}$  and we take a log-normal distribution for the host galaxy dispersion measure and repeat the calculations with the three methods discussed with 500 data points to recover a set of 100 different values for  $H_0$ . Finally, we calculate the arithmetic mean for each method and obtain the following results for  $H_0$ :  $66.21 \pm 3.46$  km/s/Mpc,  $66.10 \pm 3.46$  km/s/Mpc,  $67.30 \pm 1.89$  km/s/Mpc,  $54.34 \pm 1.57$  km/s/Mpc and  $91.84 \pm 1.82$  km/s/Mpc for arithmetic mean, median, MLE method and the  $H(z)$  reconstruction method with a linear and a power-law function, respectively. In all the methods applied to mock data, the statistical precision improves significantly, but the MLE method stands out with a value of 1.4%, which is in the order of the reports by Riess et al. (2022).

Besides the values reported for  $H_0$  with the different methods explored in this work, we highlight that the statistical precision of the predicted value of  $H_0$  increases by a factor of 2 if the set of confirmed (and localized) FRBs grows at least 5 times the current sample. More importantly, our results are consistent with other indirect methods to infer the Hubble factor today since the main observable considered here, the dispersion measure (DM), is effectively a distance from the observer and the FRB. Hence, it is unsurprising that most of our predictions lie in the range of values predicted with other indirect methods, such as CMB or BAO. Although our sample of FRBs remains in a low redshift regime ( $z_{\text{high}} \sim 1.3$ ), our results are more compatible with predictions of  $H_0$  derived with early universe probes than forecasts of this cosmological parameter made with observations in the local universe.

## CONFLICT OF INTEREST STATEMENT

The authors declare that the research was conducted in the absence of any commercial or financial relationships that could be construed as a potential conflict of interest.

## FUNDING

This work was supported by Fundaci3n Universitaria Los Libertadores programme ‘‘D3cimo Segunda (XII) Convocatoria Interna Anual de Proyectos de Investigaci3n, Creaci3n Art3stica y Cultural’’, project ‘‘Estimaci3n del espacio de par3metros para modelos difusivos cosmol3gicos a trav3s de m3todos bayesianos y de machine learning.’’ [Grant number: ING-14-24].

## ACKNOWLEDGMENTS

The authors thank Fundaci3n Universitaria Los Libertadores and Universidad ECCI for granting us the resources to develop this project. This material is based upon work supported by the Google Cloud Research Credits program with the award GCP19980904. This

research made use of `MATPLOTLIB` Hunter (2007), `SciPY` Virtanen et al. (2020) and `NUMPY` Harris et al. (2020).

## DATA AVAILABILITY

The inclusion of a Data Availability Statement is a requirement for articles published in MNRAS. Data Availability Statements provide a standardised format for readers to understand the availability of data underlying the research results described in the article. The statement may refer to original data generated in the course of the study or to third-party data analysed in the article. The statement should describe and provide means of access, where possible, by linking to the data or providing the required accession numbers for the relevant databases or DOIs.

## REFERENCES

- Aver E., Olive K. A., Skillman E. D., 2015, *Journal of Cosmology and Astroparticle Physics*, 2015, 011
- Baptista J., et al., 2023, *arXiv e-prints*, p. [arXiv:2305.07022](https://arxiv.org/abs/2305.07022)
- Bhandari S., et al., 2022, *AJ*, 163, 69
- Bhandari S., et al., 2023, *ApJ*, 948, 67
- Bhardwaj A., 2023, *Astrophysical Journal Letters*
- Bhardwaj M., et al., 2021, *ApJ*, 919, L24
- Caleb M., et al., 2023, *Monthly Notices of the Royal Astronomical Society*, 524, 2064
- Cassanelli A., 2024, *Nature*
- Connor L., et al., 2023, *ApJ*, 949, L26
- Connor L., et al., 2024, A gas rich cosmic web revealed by partitioning the missing baryons ([arXiv:2409.16952](https://arxiv.org/abs/2409.16952)), <https://arxiv.org/abs/2409.16952>
- Cordes J. M., Lazio T. J. W., 2002, *arXiv e-prints*, pp astro-ph/0207156
- Cui X.-H., et al., 2022, *Ap&SS*, 367, 66
- Deng W., Zhang B., 2014, *ApJ*, 783, L35
- Di Valentino E., et al., 2021, *Astroparticle Physics*, 131, 102605
- Driessen L. N., et al., 2023, *Monthly Notices of the Royal Astronomical Society*, 527, 3659
- Duncan A., 2022, *Journal of Astrophysics*
- Fortunato J. A. S., Bacon D. J., Hipólito-Ricardi W. S., Wands D., 2024, *arXiv e-prints*, p. [arXiv:2407.03532](https://arxiv.org/abs/2407.03532)
- Gao D. H., Wu Q., Hu J. P., Yi S. X., Zhou X., Wang F. Y., 2024
- Gordon A. C., et al., 2023a, *arXiv e-prints*, p. [arXiv:2311.10815](https://arxiv.org/abs/2311.10815)
- Gordon A. C., et al., 2023b, *The Astrophysical Journal*, 954, 80
- Hagstotz S., Reischke R., Lilow R., 2022, *MNRAS*, 511, 662
- Harris C. R., et al., 2020, *Nature*, 585, 357
- Heintz K. E., et al., 2020, *ApJ*, 903, 152
- Hoffmann J., et al., 2024, *MNRAS*, 528, 1583
- Hunter J. D., 2007, *Computing in Science & Engineering*, 9, 90
- Ibik A. L., et al., 2024, *The Astrophysical Journal*, 961, 99
- James C., 2022, *Monthly Notices of the Royal Astronomical Society*
- James C. W., Prochaska J. X., Macquart J. P., North-Hickey F. O., Bannister K. W., Dunning A., 2022, *MNRAS*, 509, 4775
- Kamionkowski M., Riess A. G., 2023, *Annual Review of Nuclear and Particle Science*, 73, 153
- Law C., 2020, *Astrophysical Journal*
- Law C., DSA-110 Collaboration 2023, in *American Astronomical Society Meeting Abstracts*. p. 239.02
- Lee-Waddell K., et al., 2023, *Publ. Astron. Soc. Australia*, 40, e029
- Liu Y., Yu H., Wu P., 2023, *The Astrophysical Journal Letters*, 946, L49
- Macquart J. P., et al., 2020, *Nature*, 581, 391
- Manchester R. N., Hobbs G. B., Teoh A., Hobbs M., 2005, *The Astronomical Journal*, 129, 1993
- McQuinn M., 2013, *The Astrophysical Journal Letters*, 780, L33
- Michilli D., et al., 2023, *The Astrophysical Journal*, 950, 134
- Nimmo K., et al., 2023, *MNRAS*, 520, 2281
- Niu C. H., et al., 2022, *Nature*, 606, 873
- Petroff E., et al., 2016, *Publ. Astron. Soc. Australia*, 33, e045
- Piratova-Moreno E. F., García L. Á., 2024, *Frontiers in Astronomy and Space Sciences*, 11, 1371787
- Planck Collaboration et al., 2020a, *A&A*, 641, A6
- Planck Collaboration et al., 2020b, *A&A*, 641, A6
- Pol N., Lam M. T., McLaughlin M. A., Lazio T. J. W., Cordes J. M., 2019, *ApJ*, 886, 135
- Prochaska J. X., Zheng Y., 2019, *Monthly Notices of the Royal Astronomical Society*, 485, 648
- Qiang D.-C., Wei H., 2020, *Journal of Cosmology and Astroparticle Physics*, 2020, 023
- Rajwade K. M., et al., 2022, *Monthly Notices of the Royal Astronomical Society*, 514, 1961
- Rajwade K. M., et al., 2024, *Monthly Notices of the Royal Astronomical Society*, 532, 3881
- Ravi V., et al., 2019, *Nature*, 572, 352
- Riess A. G., et al., 2022, *ApJ*, 934, L7
- Shannon R., Baptista J., 2024, *Astrophysics Journal*
- Shannon R. M., et al., 2024, *arXiv e-prints*, p. [arXiv:2408.02083](https://arxiv.org/abs/2408.02083)
- Sharma K., et al., 2024, Preferential Occurrence of Fast Radio Bursts in Massive Star-Forming Galaxies ([arXiv:2409.16964](https://arxiv.org/abs/2409.16964)), <https://arxiv.org/abs/2409.16964>
- Sherman M. B., et al., 2024, *The Astrophysical Journal*, 964, 131
- Tian J., et al., 2024, *Monthly Notices of the Royal Astronomical Society*, 533, 3174
- Verde L., Schöneberg N., Gil-Marín H., 2024, *ARA&A*, 62, 287
- Virtanen P., et al., 2020, *Nature Methods*, 17, 261
- Wang F. Y., Zhang G. Q., Dai Z. G., Cheng K. S., 2022, *Nature Communications*, 13, 4382
- Wang Y.-Y., Gao S.-J., Fan Y.-Z., 2025, *arXiv e-prints*, p. [arXiv:2501.09260](https://arxiv.org/abs/2501.09260)
- Wei J.-J., Melia F., 2023, *ApJ*, 955, 101
- Wu Q., Zhang G.-Q., Wang F.-Y., 2022, *MNRAS*, 515, L1
- Xu S., Weinberg D. H., Zhang B., 2021, *ApJ*, 922, L31
- Yang, Tsung-Ching Hashimoto, Tetsuya Hsu, Tzu-Yin Goto, Tomotsugu Ling, Chih-Teng Ho, Simon C.-C. Chen, Amos Y.-A. Kilerci, Ece 2025, *A&A*, 693, A85
- Yu, H. Wang, F. Y. 2017, *A&A*, 606, A3
- Zhang G. Q., Yu H., He J. H., Wang F. Y., 2020, *ApJ*, 900, 170
- Zhang X., et al., 2023, *ApJ*, 959, 89
- Zhao Z.-W., Zhang J.-G., Li Y., Zhang J.-F., Zhang X., 2022, *arXiv e-prints*, p. [arXiv:2212.13433](https://arxiv.org/abs/2212.13433)
- Zheng Z., Ofek E. O., Kulkarni S. R., Neill J. D., Juric M., 2014, *ApJ*, 797, 71
- Zhu W., Feng L.-L., 2021, *ApJ*, 906, 95

## APPENDIX A: OUR WORKING CATALOG

The data presented in Table A1 are a collection of 98 Fast Radio Bursts (FRBs) detected at various coordinates across the sky. Each entry provides detailed information about the event’s position and signal characteristics. Right Ascension (RA) and Declination (DEC) are expressed in degrees, indicating the precise sky location of each event. The observed dispersion measure ( $DM_{\text{obs}}$ ), measured  $\text{pc cm}^{-3}$ , quantifies the amount of ionized material the signal has traveled through and is accompanied by its associated error ( $\Delta DM$ ) to indicate the precision of the measurement. The table also specifies whether the FRB is a repeater (Rep), with “Y” for repeaters and “N” for single occurrences. Additionally, the redshift ( $z_{\text{host}}$ ) of the host galaxy is included, providing an estimate of the cosmological distance to the event, along with its error margin ( $\Delta z_{\text{host}}$ ). Lastly, the bibliographic reference for each detection is listed. FRB 221027A is excluded from our calculations due to ambiguity in its host galaxy localization

Table A1: 98 localized FRBs and their properties

FRB	RA (deg)	DEC (deg)	$DM_{\text{obs}}$ ( $\text{pc cm}^{-3}$ )	$\Delta DM$ ( $\text{pc cm}^{-3}$ )	Rep	$z_{\text{host}}$	$\Delta z_{\text{host}}$	Reference
121102A	82.9946	33.1479	557	2	Y	0.1927	-	2016
171020A	333.75	-19.6667	114.1	0.2	N	0.008672	-	2023
180301A	93.2292	4.6711	536	5	Y	0.3305	-	2022
180814A	65.68	73.66	189.4	3.23	Y	0.068	-	2023
180916B	29.5031	65.7168	348.8	1.62	Y	0.0337	-	2020
180924B	326.1052	-40.9	362.16	0.06	N	0.3214	-	2020; 2023b
181030A	163.2	73.74	103.5	1.62	Y	0.0039	-	2021
181112A	327.3485	-52.9709	589	0.03	N	0.4755	-	2020
181220A	348.6982	48.3421	208.66	1.62	N	0.02746	-	2023
181223C	180.9207	27.5476	111.61	1.62	N	0.03024	-	2023
190102C	322.4157	-79.4757	364.545	0.3	N	0.2913	-	2020
190110C	249.3185	41.4434	221.6	1.62	Y	0.12244	-	2024
190303A	207.9958	48.1211	223.2	1.62	Y	0.064	-	2023
190418A	65.8123	16.0738	182.78	1.62	N	0.07132	-	2023
190425A	255.6625	21.5767	127.78	1.62	N	0.03122	-	2023
190520B	240.5167	-11.2883	1204.7	4	Y	0.241	0.001	2022; 2023b
190523A	207.065	72.4697	760.8	0.6	N	0.66	2	2019
190608B	334.0199	-7.8982	340.05	0.5	N	0.1178	-	2020; 2023b
190611B	320.7455	-79.3976	332.63	0.2	N	0.3778	-	2020
190614D	65.07552	73.70674	959.2	0.5	N	0.6	-	2020
190711A	329.4195	-80.358	592.6	0.4	Y	0.5217	-	2020
190714A	183.9797	-13.021	504.13	2	N	0.2365	-	2020
191001A	323	-54.6667	507.9	0.04	N	0.234	-	2016
191106C	199.5801	42.9997	332.2	0	Y	0.10775	-	2024
191228A	344.4292	-29.5942	297.5	0.05	N	0.2432	-	2022
200120E	146.25	68.77	87.82	1.62	Y	0.0008	-	2023
200223B	82.695	288.313	201.8	-	Y	0.06024	-	2024
200430A	229.7064	12.3769	380.1	0.4	N	0.1608	-	2020
200906A	53.4958	-14.0831	577.8	0.2	N	0.3688	-	2022
201123A	263.669	-50.7672	433.55	-	Y	0.0507	-	2022
201124A	76.99	26.19	413.52	3.23	Y	0.0979	-	2022
210117A	339.9792	-16.1517	728.95	0.36	N	0.214	0.001	2023; 2023b
210320C	204.32	-15.4104	384.8	0.3	N	0.2797	-	2022; 2023b
210405I	255.3396	-49.5452	565.17	-	N	0.066	-	2023
210410D	326.0863	-79.3182	578.78	-	N	0.1415	-	2023b; 2023
210603A	10.274	21.226	500.147	0.004	N	0.1772	0.0001	2024
210807D	299.2042	-0.8143	251.9	0.2	N	0.12927	-	2022; 2023b
211127I	199.7896	-18.8246	234.83	0.08	N	0.0469	-	2022; 2023b
211203C	204.47	-31.3678	636.2	0.4	N	0.34386	-	2023b; 2024
211212A	157.6696	1.6769	206	5	N	0.0715	-	2022; 2023b
220105A	208.9642	22.4888	583	1	N	0.2785	-	2023b; 2024
220204A	278.3321	71.6157	612.2	-	N	0.4	-	2024; 2024
220207C	310.1995	72.8823	263	-	N	0.043	-	2023
220208A	319.3483	71.54	437	-	N	0.351	-	2024
220307B	350.8745	72.1924	499.328	-	N	0.248	-	2023
220310F	134.7205	73.4908	462.657	-	N	0.478	-	2023



Table A1 – continued from previous page

FRB	RA (deg)	DEC (deg)	$DM_{\text{obs}}$ (pc cm <sup>-3</sup> )	$\Delta DM$ (pc cm <sup>-3</sup> )	Rep	$z_{\text{host}}$	$\Delta z_{\text{host}}$	Reference
220319D	32.1779	71.035	110.95	0.01	N	0.011	-	2023
220330D	165.7256	71.7535	468.1	-	N	0.3714	-	2024
220418A	219.1056	70.0959	624.124	-	N	0.622	-	2023
220501C	352.3792	-32.4907	449.5	0.2	N	0.381	-	2023; 2024; 2024; 2024
220506D	318.0448	72.8273	396.651	-	N	0.3	-	2023; 2024
220509G	282.67	70.2438	269.53	10	N	0.0894	-	2023
220529A	19.10	20.63	246	-	Y	0.1839	-	2024
220610A	351	-33.5167	1458.1	0.2	N	1.016	0.002	2023a
220717A	293.3042	-19.2877	637.34	-	N	0.36295	-	2024
220725A	336.75	34.8833	290.4	0.3	N	0.1926	-	2024
220726A	75.1058	71.6018	686.55	-	N	0.361	-	2024
220825A	311.9815	72.5850	649.893	-	N	0.241	-	2024
220831A	333.0854	71.5376	1146.25	-	N	0.262	-	2024
220912A	347.2704	48.7071	219.46	0.042	Y	0.0771	-	2023
220914A	282.0568	73.3369	631.29	10	N	0.1139	-	2023
220918A	17.7413	-70.785	657	0.4	N	0.491	-	2024
220920A	240.2571	70.9188	314.977	-	N	0.158	-	2023
221012A	280.7987	70.5242	440.358	-	N	0.285	-	2023
221027A	129.6104	71.7315	452.5	-	N	0.229/0.5422	-	2024
221029A	143.8351	71.7529	1391.05	-	N	0.975	-	2024
221101B	341.4589	71.5295	490.7	-	N	0.2395	-	2024
221106A	56.7048	-25.5698	343.8	0.8	N	0.2044	-	2024; 2024
221113A	72.8406	71.6131	411.4	-	N	0.2505	-	2024
221116A	17.6617	71.5288	640.6	-	N	0.2764	-	2024
221219A	255.7773	71.6817	706.7	-	N	0.554	-	2024
230124A	233.0768	71.7273	590.6	-	N	0.094	-	2024
230216A	155.9717	1.4678	828	-	N	0.531	-	2024; 2024
230307A	177.78	71.41	608.9	-	N	0.2710	-	2024
230501A	338.5535	71.5292	532.5	-	N	0.301	-	2024; 2024
230521B	349.6785	71.5220	1342.9	-	N	1.354	-	2024; 2024
230526A	22.3646	-52.7688	316.4	0.2	N	0.157	-	2024
230626A	240.7125	71.7142	451.2	-	N	0.327	-	2024
230628A	161.8999	71.7745	345.15	-	N	0.1265	-	2024
230708A	303.2371	-55.3807	411.5	0.06	N	0.105	-	2024
230712A	170.7112	71.7794	586.96	-	N	0.4525	-	2024
230718A	127.6129	-41.0036	477	0.5	N	0.035	-	2024
230814A	335.9746	73.0259	696.4	0.05	N	0.5535	-	2024
230902A	52.3671	-47.5626	440.1	0.1	N	0.3619	-	2024
231120A	143.6169	71.7574	438.9	-	N	0.07	-	2024
231123B	240.5665	71.7156	396.7	-	N	0.2625	-	2024
231220A	122.2054	71.7217	491.2	-	N	0.3355	-	2024
231226A	155.2817	6.1294	329.9	0.1	N	0.1569	-	2024
240114A	322.0703	4.4841	527.7	-	Y	0.13	-	2024
240119A	218.1169	71.7554	483.1	-	N	0.37	-	2024
240123A	66.134	71.5965	1462	-	N	0.968	-	2024
240124A	321.9162	4.3501	526.9	-	Y	0.269	0.139	2022
240201A	149.9056	14.088	374.5	0.3	N	0.042729	-	2024
240210A	8.7796	-28.2708	283.73	0.05	N	0.0237686	-	2024
240213A	158.7613	9	357.4	-	N	0.1185	-	2024
240215A	268.4333	71.6540	549.5	-	N	0.21	-	2024
240229A	173.7346	71.7838	491.15	-	N	0.287	-	2024
240310A	17.6219	-44.4394	601.8	0.2	N	0.127	-	2024

This paper has been typeset from a  $\text{\TeX}/\text{\LaTeX}$  file prepared by the author.